Proposal to Jefferson Lab PAC 37

Proton Recoil Polarization in the ^{4}He$(e,e'p)^3$H, ^{2}H$(e,e'p)n$, and ^{1}H$(e,e'p)$ Reactions

D. Anez,[1] E. Brash,[2,*] D. Day,[3] C. Djalali,[4] R. Ent,[5] D. Gaskell,[5] S. Gilad,[6] R. Gilman,[7] D. Higinbotham,[5] G.M. Huber,[8,*] Y. Ilieva,[4] X. Jiang,[9] M. Jones,[5] C.E. Keppel,[10] M. Kohl,[10] W. Li,[8] G.J. Lolos,[8] S. Malace,[11] P.E.C. Markowitz,[12] M. Paolone,[4] Z. Papandreou,[8] C. Perdrisat,[13] E. Piasetzky,[14] I. Pomerantz,[14] A. Puckett,[9] V. Punjabi,[15] R. Ransome,[7,*] G. Rosner,[16] A.J. Sarty,[1] A. Semenov,[8] S. Strauch,[4,*] J.M. Udias,[17] L.B. Weinstein,[18] F.R. Wesselmann,[19] and X. Zhan[20]

[1] *Saint Mary's University, Halifax, NS, Canada*
[2] *Christopher Newport University, Newport News, VA*
[3] *University of Virginia, Charlottesville, VA*
[4] *University of South Carolina, Columbia, SC*
[5] *Jefferson Lab, Newport News, VA*
[6] *Massachusetts institute of Technology, Cambridge, MA*
[7] *Rutgers University, Piscataway, NJ*
[8] *University of Regina, Regina, SK, Canada*
[9] *Los Alamos National Laboratory, Los Alamos, NM*
[10] *Hampton University, Hampton, VA*
[11] *Duke University, Durham, NC*
[12] *Florida International University, Miami, FL*
[13] *College of William and Mary, Williamsburg, VA*
[14] *University of Tel Aviv, Israel*
[15] *Norfolk State University*
[16] *University of Glasgow, Glasgow, United Kingdom*
[17] *Universidad Complutense, Madrid, Spain*
[18] *Old Dominion University, Norfolk, VA*
[19] *Xavier University of Louisiana, New Orleans, LA*
[20] *Argonne National Lab, Argonne, IL*

The question whether nucleon properties are modified by the nuclear medium is a central issue in nuclear physics. For example, a wide variety of QCD-based models, including quark-meson coupling and chiral-quark soliton models, predict that the nuclear constituents change properties with increasing density. These changes are predicted to lead to observable changes in the nucleon structure functions and electromagnetic form factors. However, the experimental identification of these modifications is made difficult by the necessary presence of the nuclear medium, which also interacts with the incident and ejectile particles. Polarization transfer in quasi-elastic nucleon knockout is sensitive to the properties of the nucleon in the nuclear medium, while being influenced to a lesser degree by FSI and MEC effects than other methods.

To test these predictions, a series of recent experiments at MAMI and Jefferson Lab measured the proton recoil polarization in the ^{4}He$(\vec{e},e'\vec{p})^3$H reaction, with the most precise

data at $Q^2 = 0.8$ (GeV/c)^2 and at 1.3 (GeV/c)^2 from E03-104. These results put strong constraints on available model calculations, such that below $Q^2 = 1.3$ (GeV/c)^2 the measured ratios of polarization-transfer are successfully described in a fully relativistic calculation when including a medium modification of the proton form factors or, alternatively, by strong charge-exchange final-state interactions.

The thus constrained models, however, give very different predictions for $Q^2 \geq 1.3$ (GeV/c)^2. We therefore propose to measure the proton recoil polarization in the quasi-elastic ^{4}He$(\vec{e}, e'\vec{p})^3$H reaction at $Q^2 = 1.8$ (GeV/c)^2. The proposed data are decidedly valuable to refute either of these approaches and to shed more light on possible proton medium modifications. We request 12 days of beam for this first part of the experiment.

Medium modifications are often assumed to depend on the mean nuclear density. In other approaches, they are shown to depend explicitly upon the momentum of the bound nucleon. We are therefore proposing to study the polarization-transfer ratio in the ^{4}He$(\vec{e}, e'\vec{p})^3$H and ^{2}H$(\vec{e}, e'\vec{p})n$ reactions, to compare the knockout of tightly and weakly bound protons. We also propose to measure not only at small values of missing momentum, where models can be calibrated and reaction-mechanism effects are shown to be small, but also at larger missing momenta, where the off-shellness or virtuality of the bound proton is large. Such measurements allow us to further probe the bound nucleon electromagnetic current, including possible medium modifications of the proton electromagnetic form factor. We request 25 days to probe different virtualities of the knocked out proton in both the ^{4}He$(\vec{e}, e'\vec{p})^3$H and ^{2}H$(\vec{e}, e'\vec{p})n$ reactions in a wide range of missing momenta from -200 to $+300$ MeV/c in parallel kinematics at $Q^2 = 1.0$ (GeV/c)^2.

For both Q^2 values, we also propose to take additional $\vec{e}p$ data as reference point for elastic electron scattering on a free proton.

---

* co-spokesperson

CONTENTS

I. PHYSICS MOTIVATION

A. Introduction

The underlying theory of strong interactions is Quantum ChromoDynamics (QCD), yet there are no ab-initio calculations of nuclei available. Nuclei are effectively and well described as clusters of protons and neutrons held together by a strong, long-range force mediated by meson exchange, whereas the saturation properties of nuclear matter arise from the short-range, repulsive part of the strong interaction [1]. At nuclear densities of about 0.17 nucleons/fm^3, nucleon wave functions have significant overlap. In the chiral limit, one expects nucleons to lose their identity altogether and nuclei to make a transition to a quark-gluon plasma [2]. This phase transition is extensively being studied at the RHIC facility.

Within QCD, there is no known way to derive anything like an atomic nucleus in which the constituents do not change as the mean density (or temperature) goes away from zero [3]. The discovery of the nuclear EMC effect, the depletion of the deep inelastic structure function observed in the valence quark regime, almost twenty years ago brought the subjects of quarks into nuclear physics with great impact. The EMC effect is also subject of a broad experimental program in Hall C, where the F_2 structure function in inclusive electron scattering off nuclei at large Q^2 has been measured in a series of experiments: E89-008 [4], E02-019 [5], and most recently in E03-103 [6]. The latter is a precision measurement of the EMC effect in both few-body nuclei and heavy nuclei [7]. Still, the specific causes of the modifications observed in the nuclear structure functions have not yet been identified with

certainty [8]. Miller and Smith [9] argue that the depletion is due to some interesting effect involving dynamics beyond the conventional nucleon-meson treatment of nuclear physics. One such explanation is a medium modification of bound nucleon structure. A variety of models predict measurable deviations from the free space nucleon form factor ratio G_E/G_M in the nuclear medium: A calculation by Lu *et al.* [10, 11], using a quark-meson coupling (QMC) model, suggests a measurable deviation from the free-space electromagnetic form factor over the four-momentum-transfer squared Q^2 range $0.0 < Q^2 < 2.5$ $(\mathrm{GeV}/c)^2$. Similar measurable effects have been calculated in a light-front-constituent quark model by Frank *et al.* [12], a modified Skyrme model by Yakshiev *et al.* [13], a chiral quark-soliton model (CQS) by Smith and Miller [14], and the Nambu-Jona-Lasinio model [15, 16]. See Fig. 1 for a comparison of the QMC- and CQS-model results. Medium modifications of nucleon

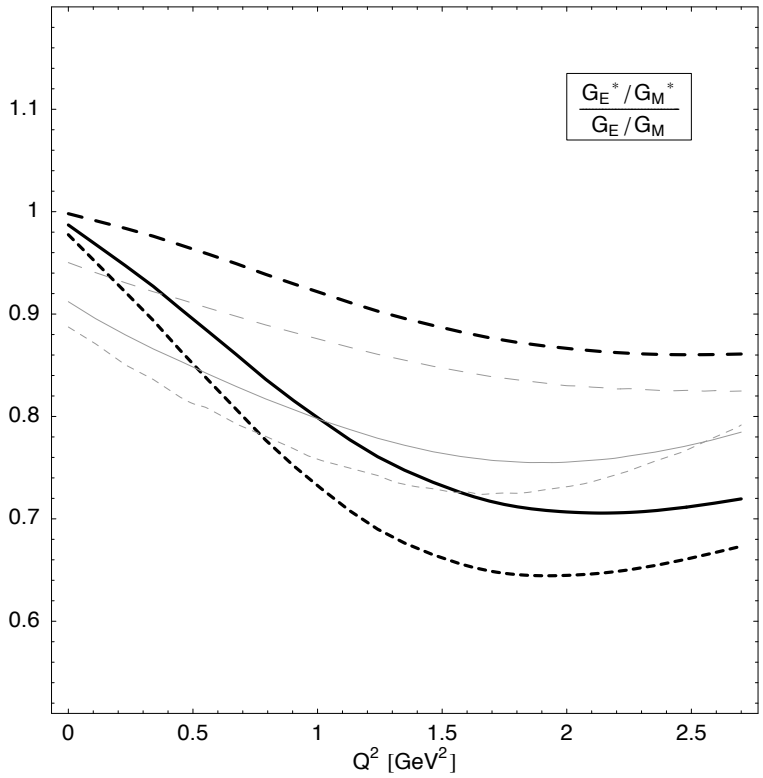

FIG. 1. The double ratio, $(G_E(Q^2)/G_M(Q^2))_{\mathrm{medium}}/(G_E(Q^2)/G_M(Q^2))_{\mathrm{free}}$, of the electric to magnetic form factors in nuclear matter and in the vacuum from the CQS model [14] (heavy) and the QMC model [10, 11] (light). Three densities are shown: $0.5\rho_0$ (long dashes), $1.0\rho_0$ (solid), and $1.5\rho_0$ (short dashes). Figure taken from [14].

properties in nuclear matter and finite nuclei have been also discussed by Wen and Shen [17]. Furthermore, the nuclear modification of axial form factors [18, 19] also may be measured. The connection between the modifications induced by the nuclear medium of the nucleon form factors and of the deep inelastic structure functions is discussed by Liuti [20] using the concept of generalized parton distributions (GPDs). Guzey *et al.* [21] have studied incoherent deeply virtual Compton scattering (DVCS) on ^{4}He in the $^4\mathrm{He}(e, e'\gamma p)X$

reaction, which probes medium-modifications of the bound nucleon GPDs and elastic form factors. They have also investigated medium modification of the quark contribution to the spin sum rule [22]. These calculations are generally consistent with present constraints on possible medium modifications for both the electric form factor (from the Coulomb Sum Rule, for $Q^2 < 0.5$ (GeV/c)^2 [23–25]) and the magnetic form factor (from a y-scaling analysis [26] for $Q^2 > 1$ (GeV/c)^2), and limits on the scaling of nucleon magnetic moments in nuclei [27].

Thus, although models using free nucleons and mesons as quasi-particles are successful in the description of many aspects of nuclear physics, one may expect that, under certain circumstances, their use is a highly uneconomical approach, especially given that these are not the fundamental entities of the underlying theory. The use of medium-modified nucleons as quasi-particles may be a better choice. To experimentally demonstrate any modification of the nucleon form factors, one is required to have excellent control over the reaction mechanism effects [28]. The nucleus, as a bound many-body quantum system, has inherent many-body effects, such as meson-exchange currents (MEC) and isobar configurations (IC). In addition, when probing nuclear structure one has to deal with final-state interactions (FSI). A change in the spatial structure of the nucleon, as expressed in medium modifications of the nucleon form factors, implies that one treats observed medium effects as density dependent one-body effects, and assumes that the major part of the many-body effects are therein incorporated. If medium-modified nucleon form factors are defined, in principle medium-modified many body effects are also required in order to perform a rigorous calculation of nuclear structure.

There is no experimental way to distinguish between both approaches: the notion of medium modification of single particle properties like, *e.g.*, the electromagnetic form factors of a nucleon, in a nuclear environment is a purely theoretical concept. Thus, distinguishing possible changes in the spatial structure of nucleons embedded in a nucleus from more conventional many-body effects is only possible within the context of a model. We argue the quasi-elastic proton knockout in the proposed ^{4}He$(\vec{e}, e'\vec{p})^3$H and ^{2}H$(\vec{e}, e'\vec{p})n$ reactions to be the most directly accessible experimental method to challenge conventional meson-nucleon modeling where these conventional effects are suppressed.

B. Recoil Polarization in Quasi-Elastic Electron Scattering

One of the most intuitive methods to investigate the properties of nucleons inside nuclei is quasi-elastic scattering off nuclei. Since the charge and magnetic responses of a single nucleon are quite well studied from elastic scattering experiments, measuring the same response from quasi-elastic scattering off nuclei and comparing with a single nucleon is likely to shed light on the question. Polarization transfer in quasi-elastic nucleon knockout is sensitive to the properties of the nucleon in the nuclear medium, including possible modification of the nucleon form factor and/or spinor. This can be seen from free electron-nucleon scattering, where the ratio of the electric to magnetic Sachs form factors, G_E and

G_M, is given by [29, 30]:

$$\frac{G_E}{G_M} = -\frac{P'_x}{P'_z} \cdot \frac{E_e + E_{e'}}{2m_p} \tan(\theta_e/2), \tag{1}$$

where P'_x and P'_z are the transverse and longitudinal transferred polarizations; see Fig. 2. The beam energy is E_e, the energy (angle) of the scattered electron is $E_{e'}$ (θ_e) and m_p is the proton mass. This relation was extensively used to extract G_E/G_M for the proton, see *e.g.* [31–35].

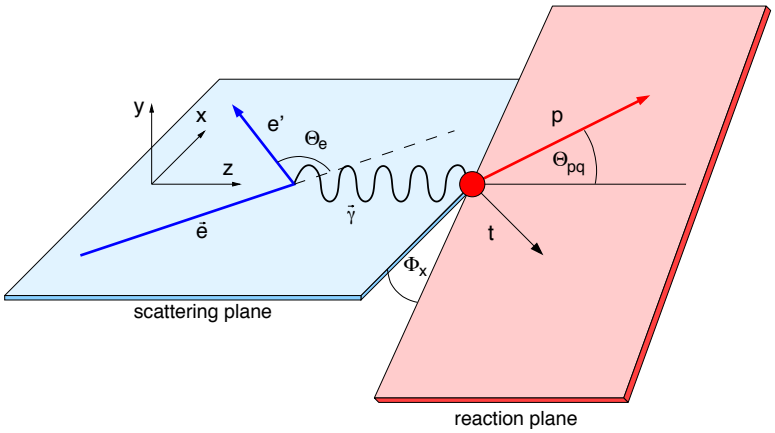

FIG. 2. Coordinate system used to define the components of the recoil proton polarization in the ^{4}He$(\vec{e}, e'\vec{p})^3$H reaction. The z axis is along the momentum transfer, the x axis is in the scattering plane perpendicular to the momentum transfer $\vec{q}$ and the y axis is perpendicular to the scattering plane, forming a right-handed system.

When such measurements are performed on a nuclear target in quasi-elastic kinematics, the experimental results for the polarization-transfer ratio are conveniently expressed in terms of the polarization double ratio

$$R = \frac{(P'_x/P'_z)_A}{(P'_x/P'_z)_{^1\mathrm{H}}}, \tag{2}$$

where the polarization-transfer ratio for the quasi-elastic proton knockout $A(\vec{e}, e'\vec{p})$ reaction is normalized to the polarization-transfer ratio measured in elastic ^{1}H$(\vec{e}, e'\vec{p})$ scattering in the identical setting in order to emphasize differences between the in-medium compared to the free values. Such a double ratio cancels also nearly all experimental systematic uncertainties. A proper interpretation of the results requires accounting for such effects as FSI and MEC. At high momentum transfer, however, the contribution of many-body and rescattering mechanisms are strongly suppressed and spin observables provide us with a way to study the behavior of the nucleon form factors in the nuclear medium [36].

C. Previous Experimental Results

JLab Experiment E89-033 was the first to measure the polarization transfer in a complex nucleus, ^{16}O [37]. The results are consistent with predictions of relativistic calculations

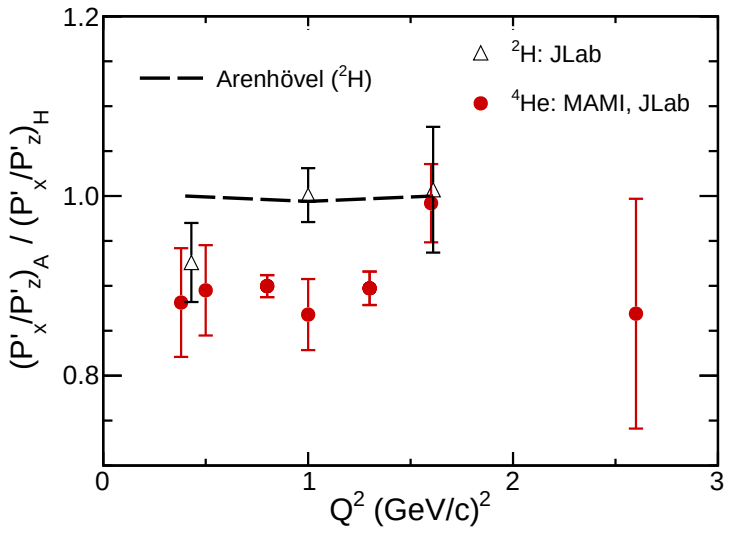

FIG. 3. Bound-to-free polarization-transfer double ratio R at low missing momenta for $^2\mathrm{H}(\vec{e},e'\vec{p})n$ (open triangles) from [41] and for $^4\mathrm{He}(\vec{e},e'\vec{p})^3\mathrm{H}$ (closed circles) from [42–44] as a function of Q^2. The curve shows a result of a calculation by Arenhövel (dashed line) for deuterium.

based on the free proton from factor with an experimental uncertainty of about 18%. Polarization transfer has been used previously to study nuclear medium effects in deuterium [38–40]. Within statistical uncertainties, no evidence of medium modifications was found. More recently, polarization-transfer data on ^{2}H were measured in JLab experiment E89-028 [41], under conditions very similar to those for experiment E93-049 on ^{4}He. Realistic calculations to describe this reaction were performed by Arenhövel. Experimental results (open triangles) for the ^{2}H-to-^{1}H polarization-transfer double ratio, along with the results of a calculation by Arenhövel (dashed curve), are shown in Fig. 3. Arenhövel's full calculation describes the ^{2}H data well. As the sampled density is small and the bound proton in ^{2}H is nearly on mass-shell, it is not surprising that there are no indications for medium modifications of the proton electromagnetic form factors in the ^{2}H data.

One might expect to find larger medium effects in ^{4}He, with its significantly higher density. Indeed, recent Jefferson Lab Experiment E03-103 has measured the EMC effect for various nuclei and results indicate that the nuclear dependence of the cross section is nearly identical for ^{4}He and ^{12}C [7]. Although estimates of the many-body effects in ^{4}He may be more difficult than in ^{2}H, calculations for ^{4}He indicate they are small [36]. The first $^4\mathrm{He}(\vec{e},e'\vec{p})^3\mathrm{H}$ proton recoil-polarization measurements were performed at MAMI at $Q^2 = 0.4$ (GeV/c)^2 [42] and at Jefferson Lab Hall A at $Q^2 = 0.5$, 1.0, 1.6, and 2.6 (GeV/c)^2, E93-049 [43]. Experiment E03-104 extended these measurements with two high-precision points at $Q^2 = 0.8$ and 1.3 (GeV/c)^2 [44]. The results are shown in Fig. 3 (solid points). The missing-mass technique was used to identify ^{3}H in the final state. For a reliable interpretation of the experimental data it is imperative to have good control over

conventional many-body effects in the reaction. All these data were thus taken in quasi-elastic kinematics at low missing momentum with symmetry about the three-momentum-transfer direction to minimize these effects. Furthermore, they can be studied with the induced polarization, P_y, which is a direct measure of final-state interactions. Induced-polarization data were taken simultaneously to the polarization-transfer data.

Figure 4 shows the results for P_y. The induced polarization is small at the low missing momenta in this measurement. The sizable systematic uncertainties are due to possible instrumental asymmetries. Dedicated data were taken during E03-104 to study these and help significantly reduce systematic uncertainties in the extraction of P_y. The data are compared with results of a relativistic distorted-wave impulse approximation (RDWIA) calculation by the Madrid group [47–49]. In this model FSI are incorporated using an updated version of the RLF relativistic optical potentials [51, 52] that distort the final nucleon wave function; the MRW optical potential of [53], used in [44], does not yield an as good description of P_y as the modified RLF potential shown here. Charge-exchange terms are not taken into account in the Madrid RDWIA calculation; preliminary studies show, however, that there are of small effect in this model [54]. Calculations are shown for choices of *cc1* and *cc2* current operators as defined in [55]. The choice *cc1* yields the largest prediction for P_y in absolute value and describes the data well; possibly hinting at the importance of the lower spinor components in this relativistic calculation; see [49]. We note that these RDWIA calculations provide also good descriptions of, e.g., the induced polarizations as measured at Bates in the ^{12}C(e,e$'\vec{p}$) reaction [49, 56] and of A_{TL} in ^{16}O$(e, e'p)$ as previously measured at JLab [57]. While the polarization-transfer observables are expected to be sensitive to possible nucleon medium modifications, results of the RDWIA calculation including medium-modified form factors show only some small effect on the induced polarization. The data are also compared with the results of a calculation from Schiavilla *et al.* [46] (shaded band). That model uses variational wave functions for the bound three- and four-nucleon systems, non-relativistic MEC and free nucleon form factors. The FSIs are treated within the optical potential framework and include both spin-independent and spin-dependent charge-exchange terms which play a crucial role in the prediction of P_y. Note that the charge-exchange term gives the largest contribution to Schiavilla's calculation of P_y. This model describes the data well after being constrained to the new data from E03-104.

The ^{4}He polarization-transfer double ratio is shown in Figure 5. The recent data from E03-104 (filled circles) [44] are consistent with the previous data from E93-049 [43] and MAMI [42] (open symbols). The polarization-transfer ratio (P'_x/P'_z) in the $(\vec{e}, e'\vec{p})$ reaction on helium is significantly different from those on deuterium or hydrogen. The helium data are compared with results of the same RDWIA calculations by the Madrid group [47–49] (dotted curves) as in Fig. 4. MEC are not explicitly included in the Madrid calculation. Predictions by Meucci *et al.* [58] show that the two-body current (the seagull diagram) effects on the polarization-transfer ratio are generally small; less than 3 % at low missing momenta and visible only at high missing momenta. It can be seen that the Madrid RDWIA calculation (dotted curves) overpredicts the data. The agreement of the Madrid model with

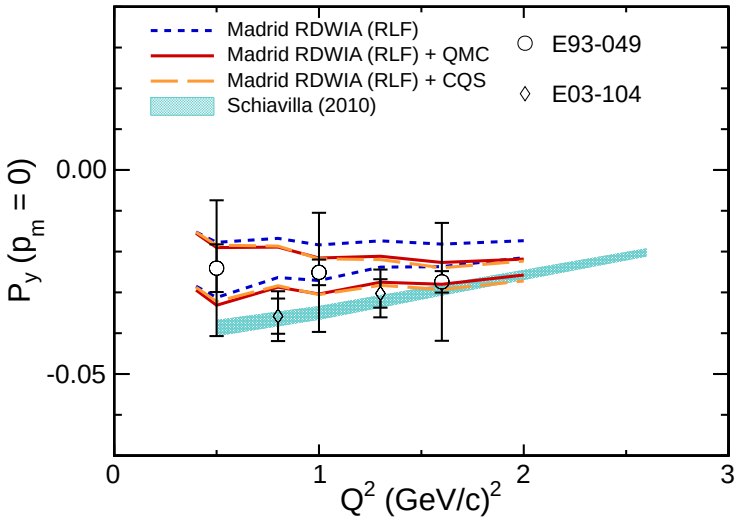

FIG. 4. ^{4}He$(e,e'\vec{p})^3$H induced polarization data from Jefferson Lab experiment E93-049 [43] along with results from experiment E03-104 [45]. The data are compared to calculations from Schiavilla *et al.* [46] and the Madrid group [47–49] using the *cc1* (lower set of curves) and *cc2* (upper set of curves) current operators. In-medium form factors from the QMC [10] (solid curve) and CQS [14] (dashed curve) models were used in two of the Madrid calculations. Note that the comparison is made for missing momentum $p_m \approx 0$ and that the experimental data have been corrected for the spectrometer acceptance for this comparison.

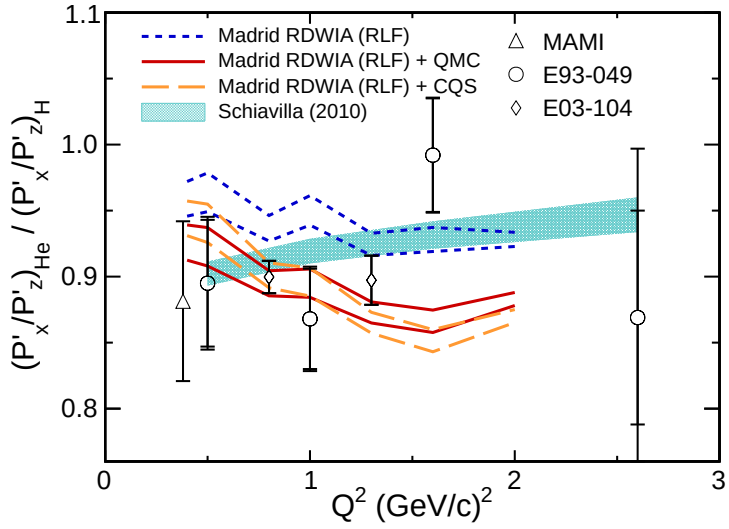

FIG. 5. ^{4}He$(\vec{e},e'\vec{p})^3$H polarization-transfer double ratio R as a function of Q^2 from Mainz [42] and Jefferson Lab experiments E93-049 [43] (open symbols) and E03-104 [44] (filled circles). The data are compared to calculations from the Madrid group [47–49], using the *cc1* (lower set of curves) and *cc2* (upper set of curves) current operators, and Schiavilla *et al.* [46] as in Fig. 4. Not shown are a relativistic Glauber model calculation by the Ghent group [50] and results from Laget [36] which give both a value of $R \approx 1$.

the polarization-transfer data is improved after including the density-dependent medium-modified form factors from the QMC [10] or CQS [14] models in the RDWIA calculation (solid and dashed curves). This agreement has been interpreted as possible evidence of proton medium modifications [43]. An alternative interpretation of the observed suppression of the polarization-transfer ratio is offered within the more traditional calculation by Schiavilla *et al.* [46] (shaded band). Schiavilla's calculation uses free nucleon form factors and explicitly includes MEC effects which are suppressing R by almost 4%.

Currently, the ^{4}He$(\vec{e},e'\vec{p})^3$H polarization-transfer data can be well described by either the inclusion of medium-modified form factors or strong charge-exchange FSI in the models. The difference in the modeling of final-state interactions is the origin of the major part of the difference between the results of the calculations by Madrid *et al.* [47–49] and Schiavilla *et al.* [46] for the polarization observables. Optical potentials in these models have now been constrained to the new induced polarization data from E03-104.

II. PROPOSED EXPERIMENT

A. Overview

In this experiment, we propose to take production data on three targets: ^{1}H, ^{2}H, and ^{4}He. The data on hydrogen will provide the reference point for elastic electron scattering on a free proton. As the induced polarization P_y from hydrogen is zero in the one-photon-exchange approximation, these data will also help to understand the instrumental asymmetries of the Focal Plane Polarimeter (FPP). Case in point is our recent experiment E03-104 [45] where ep data have been essential to reduce the systematic uncertainty on the P_y extraction by a factor of four when compared to previous, similar measurements from E93-049.

The data on deuterium will provide a link between free ep scattering and quasi-elastic proton knockout in ^{4}He. The ^{2}H and ^{4}He data have in common that in both cases the reaction takes place on a bound, off-shell nucleus. While the proton in helium is tightly bound in a nuclear medium which is much denser than that in deuterium similar nucleon virtualities can be reached in both, the ^{2}H$(e,e'p)n$ and ^{4}He$(e,e'p)^3$H reactions at larger missing momenta; see Fig. 6. Here, the proton virtuality is defined as $v = p^2 - m_p^2$, where p is the four-momentum of the bound proton. In impulse approximation $p^2 = (m_A - E_m)^2 - p_m^2$, where E_m and p_m are respectively the missing energy and momentum in the $A(e,e'p)$ reaction. The origin of medium effects, as density dependent or bound-nucleon-momentum dependent, will thus become apparent in a comparison between both of these data.

The target nucleus ^{4}He is optimal for further study since its relative simplicity allows for realistic microscopic calculations and since its high density enhances any possible medium effects. Also, a variety of calculations for the ^{4}He$(\vec{e},e'\vec{p})^3$H reaction indicate that polarization transfer observables are influenced little by FSI and MEC effects, amounting to only about a 10% correction [36, 47–49, 59]. If, instead of ^{4}He, one would be able to use a heavier target nucleus, or any nuclear transition, that effectively probes some higher nuclear

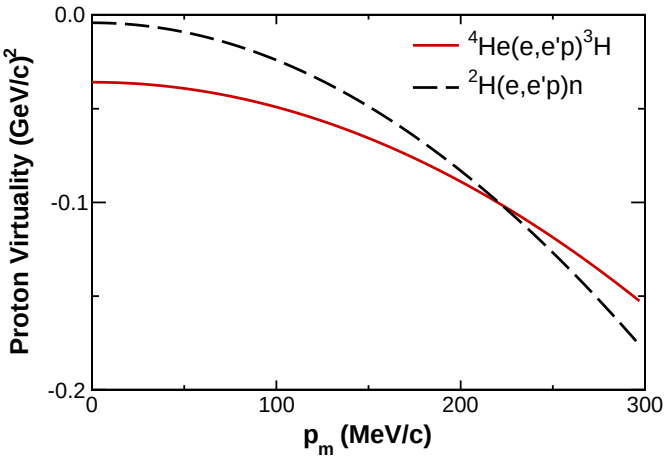

FIG. 6. The proton virtuality is a function of the missing momentum in the $A(e,e'p)$ reaction. Similar proton virtualities are experimentally accessible in the $^4\mathrm{He}(\vec{e},e'\vec{p})^3\mathrm{H}$ and $^2\mathrm{H}(\vec{e},e'\vec{p})n$ reactions at larger missing momenta.

density region than in the $^4\mathrm{He}(\vec{e},e'\vec{p})^3\mathrm{H}$ reaction, this would be worthwhile. However, in terms of the effective density sampled in the $(e,e'p)$ reaction, ^{4}He is only marginally less dense than heavier nuclei. The average density as sampled in, e.g., the $^{16}\mathrm{O}(e,e'p)$ reaction is only slightly larger than that for the $^4\mathrm{He}(e,e'p)$ reaction (which is about 0.25 times the nuclear matter density), whereas microscopic calculations may be more troublesome, and experimental rates are smaller. Furthermore, Coulomb corrections are more of an issue for heavier nuclei. On the technical side, ^{4}He can easily withstand high beam currents (possible target boiling effects do not affect the polarization measured). Therefore, ^{4}He remains the target of choice.

The proposed measurement has two parts. As first part we propose to measure one new high-precision data point of the ^{4}He polarization-transfer double ratio at $Q^2 = 1.8$ (GeV/c)^2; see Fig. 7. Current quite different, state of the art, models which employ free nucleon form factors (Madrid RDWIA and Schiavilla) agree in their predictions above $Q^2 = 1.3$ (GeV/c)^2 where ambiguities in the choice of the current operator become smaller. Including medium modifications of the proton form factors in the Madrid calculations, on the other hand, results in an easily observable reduction of the polarization-transfer double ratio of at least 5%. A new, high precision data point at $Q^2 = 1.8$ (GeV/c)^2 will be decidedly valuable to refute either of these approaches: If a new result agrees with that set of calculations without the need of medium modified form factors it will seriously challenge the present models of in-medium effects. If, on the other hand, the new data will agree with those predictions which include the QMC or CQS form factors it is very hard to see how this observation can be reconciled in the other models given the already tight constrains from E03-104.

As second part we propose an extensive study of the proton recoil-polarization observables as a function of missing momentum or proton virtuality in both the $^4\mathrm{He}(\vec{e},e'\vec{p})^3\mathrm{H}$ and $^2\mathrm{H}(\vec{e},e'\vec{p})n$ reactions at $Q^2 = 1.0$ (GeV/c)^2. On the one hand, the cross section and the

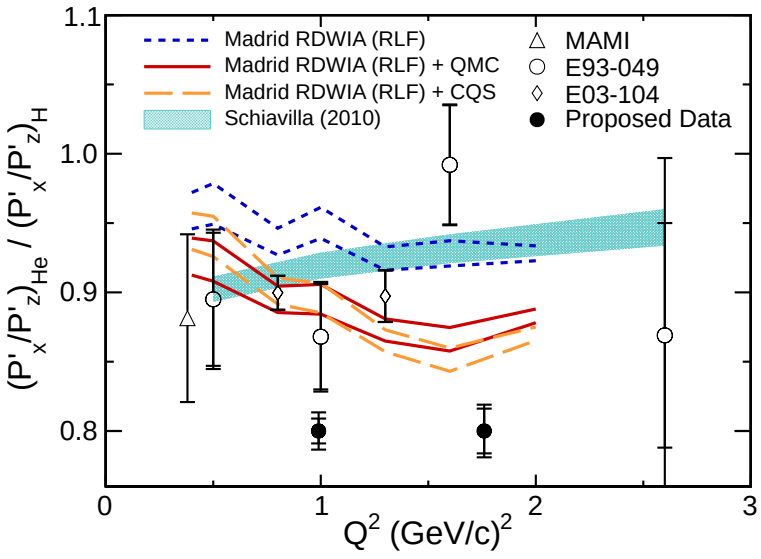

FIG. 7. Previous polarization-transfer double ratios for ^{4}He$(\vec{e},e'\vec{p})^3$H (open symbols) along with arbitrarily placed proposed data (solid points). The proposed data are integrated over a missing momentum range of $|p_m| < 100$ MeV/c for 1.0 (GeV/c)^2 and over $|p_m| < 175$ MeV/c for 1.8 (GeV/c)^2. The data are compared with various model calculations; as in for Fig. 4. The inner error bar reflects statistical uncertainties only, while the outer bar includes the effect of projected experimental systematic uncertainties.

magnitude of the polarization-transfer coefficients at $Q^2 = 1.0$ (GeV/c)^2 are large enough to allow for adequate precision; a similar measurement at $Q^2 = 1.5$ (GeV/c)^2 would require, depending on the beam energy, about four to six times more beam time. On the other hand, the value of $Q^2 = 1.0$ (GeV/c)^2 is also sufficiently high that RDWIA and Schiavilla approaches begin to yield similar results and modern Eikonal descriptions [60] begin to work. Ciofi degli Atti *et al.* [61] argue that the modification of the wave function of the bound nucleon in a nucleus should strongly depend on the momentum of the nucleon. Figure 8 shows R as a function of the proton virtuality. The same proton virtuality can be accessed in the ^{4}He$(\vec{e},e'\vec{p})^3$H and ^{2}H$(\vec{e},e'\vec{p})n$ reactions within the same experimental setup for nucleon knockout at a missing momentum of about 220 MeV/c. At these missing momenta both reactions are thus suited to address the question whether medium modifications, as often considered, depend on the mean nuclear density, or explicitly upon the momentum of the nucleon. We are therefore proposing to study the polarization-transfer ratio not only at small values of missing momentum, where models can be calibrated and reaction-mechanism effects are shown to be small, but also at larger values of missing momentum, in order to test this argument.

These expected data could put much stronger constraints on possible medium effects, including the medium-modification of the proton structure, than the previous data do. The coverage and expected precision of these data as a function of proton virtuality are

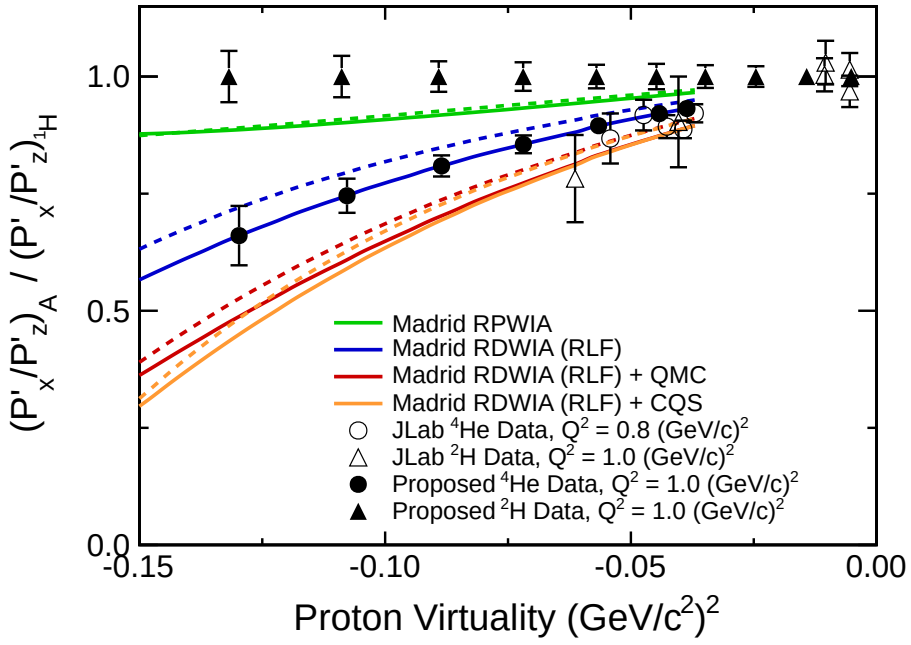

FIG. 8. Polarization-transfer ratio P'_x/P'_z from bound nucleon knockout off ^{4}He (solid circles) and ^{2}H (open triangles) compared to P'_x/P'_z from elastic ep scattering as a function of proton virtuality. The curves are various calculations using the model of Udias *et al.* for the reaction on ^{4}He and current operators $cc1$ (solid curves) and $cc2$ (dotted curves). The points indicate previous data [41, 44] and the statistical uncertainties of the proposed data and which are arbitrarily placed on the RDWIA ($cc1$) curve for ^{4}He and at $R = 1$ for ^{2}H.

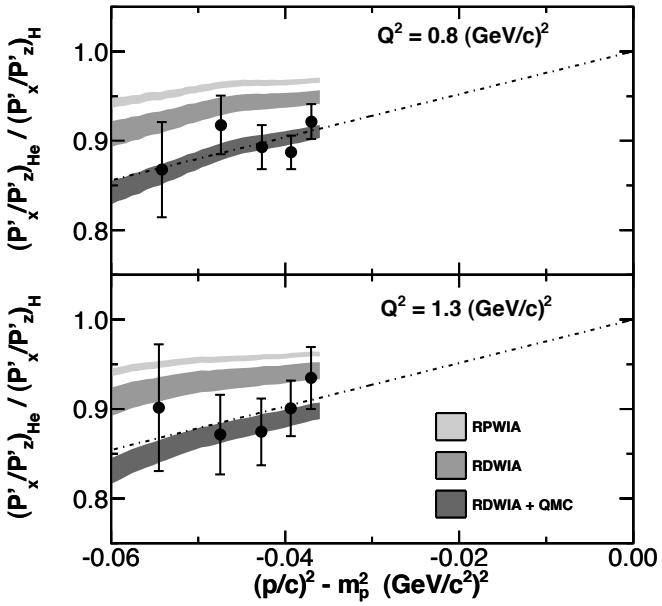

FIG. 9. The double ratio R versus proton virtuality for Q^2= 0.8 and 1.3 $(\mathrm{GeV}/c)^2$ [44]. The dashed line is a linear fit to the data constrained to have a y intercept value of one at zero proton virtuality. The bands represent RPWIA (light grey), RDWIA calculations (grey), and RDWIA + QMC calculations (dark grey) [47–49]. Figure taken from [44].

shown in Fig. 8 for the $Q^2 = 1.0$ (GeV/c)^2 setting. The proposed ^{4}He$(\vec{e}, e'\vec{p})^3$H data substantially expand the range covered by our previous experiment E03-104 [44], Fig. 9, while the proposed ^{2}H$(\vec{e}, e'\vec{p})n$ data cover the full range from nearly on-shell up to the large values of proton virtuality reached in ^{4}He, far exceeding earlier data of Hu *et al.* [41]. We will concentrate on the $x > 1$ region where FSI effects are found to be restricted and which is most suitable for probing the bound nucleon electromagnetic current [60].

Polarization transfer in the quasi-elastic proton-knockout reaction is arguably one of the most direct experimental methods to identify nuclear-medium changes to nucleon properties, which are predicted by QCD-based models, as other conventional medium effects, such as many-body currents and final state interactions, are suppressed. Furthermore, the possible role of FSI in the interpretation of these data can be constrained by our data on the induced polarization P_y.

In continuation of the series of our earlier experiments at MAMI and JLab Hall A (E93-049 and E03-104), we propose to measure the proton-recoil polarization observables in the ^{4}He$(\vec{e}, e'\vec{p})^3$H, ^{2}H$(\vec{e}, e'\vec{p})n$, and ^{1}H$(\vec{e}, e'\vec{p})$ reactions in Hall C. Key features of the new experiment include:

1. We propose to measure two new high-precision data points of the polarization-transfer double ratio at $Q^2 = 1.0$ and 1.8 (GeV/c)^2 to study thoroughly the Q^2 dependence of possible modifications of in-medium proton form factors; Fig. 7.

2. We propose a significantly improved proton virtuality coverage at $Q^2 = 1.0$ (GeV/c)^2 to study the expected strong dependence of medium effects on the momentum of the bound nucleon; Fig. 8.

   (a) Here, we propose to measure a range covering about $p_m = -200$ MeV/c to $+300$ MeV/c in parallel kinematics, with special emphasis on the $x > 1$ region.

   (b) We propose to take data from ^{4}He$(\vec{e}, e'\vec{p})^3$H and ^{2}H$(\vec{e}, e'\vec{p})n$ to compare knock-out data of tightly and weakly bound protons to further probe the bound nucleon electromagnetic current including possible medium modifications of the proton electromagnetic form factor. Modern calculations are readily available for both reactions; *e.g.* [46–49, 60, 62].

B. Kinematics

The proposed settings for this experiment are listed in Table I, all of which are for the proton detection along the q-vector (parallel kinematics). The "standard 12 GeV tune" 1-pass and 2-pass beam energies are used. Since we expect relatively little demand for these standard low beam energies, we hope their use will simplify the scheduling of the experiment. Since we propose to detect protons for angles as large as 57.4°, the HMS must be used for proton detection and the SHMS for electron detection [63]. Thus, the FPP will be installed in the HMS for this experiment, which poses no technical difficulties.

For each of the settings listed in Table I, HMS+SHMS simulations were performed with SIMC, using the SHMS matrix elements updated by Dave Gaskell in December, 2009. Acceptance cuts of HMS $|\delta p/p| < 8\%$, HMS $|x'_{target}| < 60$ mrad, and SHMS $-10\% < \delta p/p < 22\%$ were applied. The simulated SHMS+HMS coincidence acceptances for the proposed $Q^2 = 1.0$ (GeV/c)^2 settings are shown in Fig. 10.

TABLE I. Proposed parallel kinematics. The scattered electron will be detected in the SHMS and the proton spin analyzed in the HMS FPP. For each Q^2, seven hydrogen elastics settings are planned, spanning the range of HMS momentum indicated.

Target	E_e	p_m	$E_{e'}$	$\theta_{e'}$	p_p	θ_p	Current	Time
	(GeV)	(GeV/c)	(GeV)	(deg)	(GeV/c)	(deg)	(μA)	(hr)
$Q^2 = 1.0$ (GeV/c)^2 Settings								
^{4}He	2.250	+0.220	1.902	27.98	0.839	57.40	75	250
		+0.140	1.836	28.49	0.942	53.98	75	48
		0.0	1.686	29.75	1.148	46.80	75	48
^{2}H	2.250	+0.220	1.902	27.97	0.839	57.42	75	150
		+0.140	1.849	28.38	0.937	54.68	75	16
		0.0	1.714	29.50	1.135	48.05	50	6
^{1}H	2.250	0.0	1.717	29.48	1.021 – 1.296	48.20	25	7 × 3.0
$Q^2 = 1.8$ (GeV/c)^2 Settings								
^{4}He	4.400	0.0	3.401	19.97	1.673	43.99	75	225
^{1}H	4.400	0.0	3.441	19.85	1.484 – 1.885	45.12	75	7 × 6.0

^{4}He Q^2 Distribution The settings in Table I will allow the precision of the polarization-transfer double ratios R at Q^2 =1.0 and 1.8 (GeV/c)^2 to be greatly improved. Projected uncertainties are shown in Fig. 7. For the purposes of these estimates, Q^2 binning cuts of $0.85 < Q^2 < 1.15$ (GeV/c)^2, and $1.60 < Q^2 < 2.00$ (GeV/c)^2, were applied, yielding ratio measurements at mean Q^2 values of 0.99 and 1.76 (GeV/c)^2. Missing momentum cuts, $|p_m| < 100$ MeV/c at $Q^2 = 1.0$ (GeV/c)^2 and $|p_m| < 175$ MeV/c at $Q^2 = 1.8$ (GeV/c)^2, would be placed to ensure that the missing momenta for each point is small and averages to nearly zero.

Virtuality Distributions We propose to take additional ^{2}H and ^{4}He data at $Q^2 = 1.0$ (GeV/c)^2 spanning a wide range of missing momentum (or proton virtuality) in parallel kinematics. The justification of these studies is to probe for momentum dependent effects upon the wave function of the bound nucleon. At this Q^2, the data come in relatively quickly. Several SHMS+HMS coincidence settings are required, where both the energy and momentum transfer are adjusted to ensure that Q^2 and p_m are fixed at the required values.

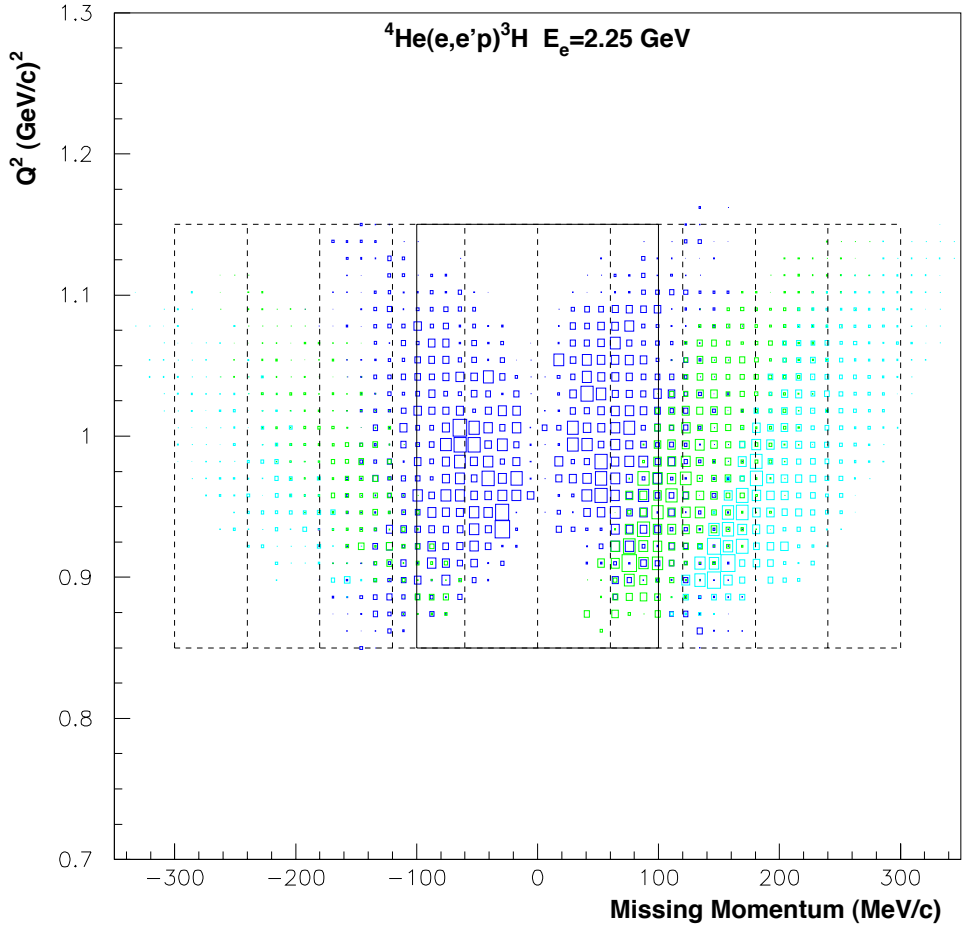

FIG. 10. Simulated ^{4}He$(e,e'p)^3$H kinematic coverage for the $Q^2 = 1.0$ (GeV/c)^2 settings listed in Table I. The respective HMS settings are indicated by color: Blue: $p_m = 0$, Green: $p_m = +0.140$ MeV/c, Cyan: $p_m = +0.220$ MeV/c. All acceptance cuts listed in the text, as well as a missing mass cut to select the $t + p$ final state, are applied. The solid and dashed lines indicate a possible binning of these data.

These p_m settings are given in the third column of Table I and the expected event yield for the ^{4}He data is shown in Fig. 11. Our simulations indicate that the deuterium coincidence rate (for same unit luminosity, and after cuts) is a factor of 10 higher than ^{4}He at $p_m = 0$, with the ratio dropping to about 1.5 at large missing momentum. A Q^2 binning cut of $0.85 < Q^2 < 1.15$ (GeV/c)^2 was applied, and the data were divided into bins of proton virtuality from -0.15 (GeV/c^2)^2 to 0. Projected uncertainties for the polarization transfer ratio are shown in Fig. 8. In order to make the most definitive statement possible on the polarization-transfer ratio at large proton virtualities in a given beam time, we have decided to concentrate the data acquisition to $x > 1$, corresponding to positive missing momenta.

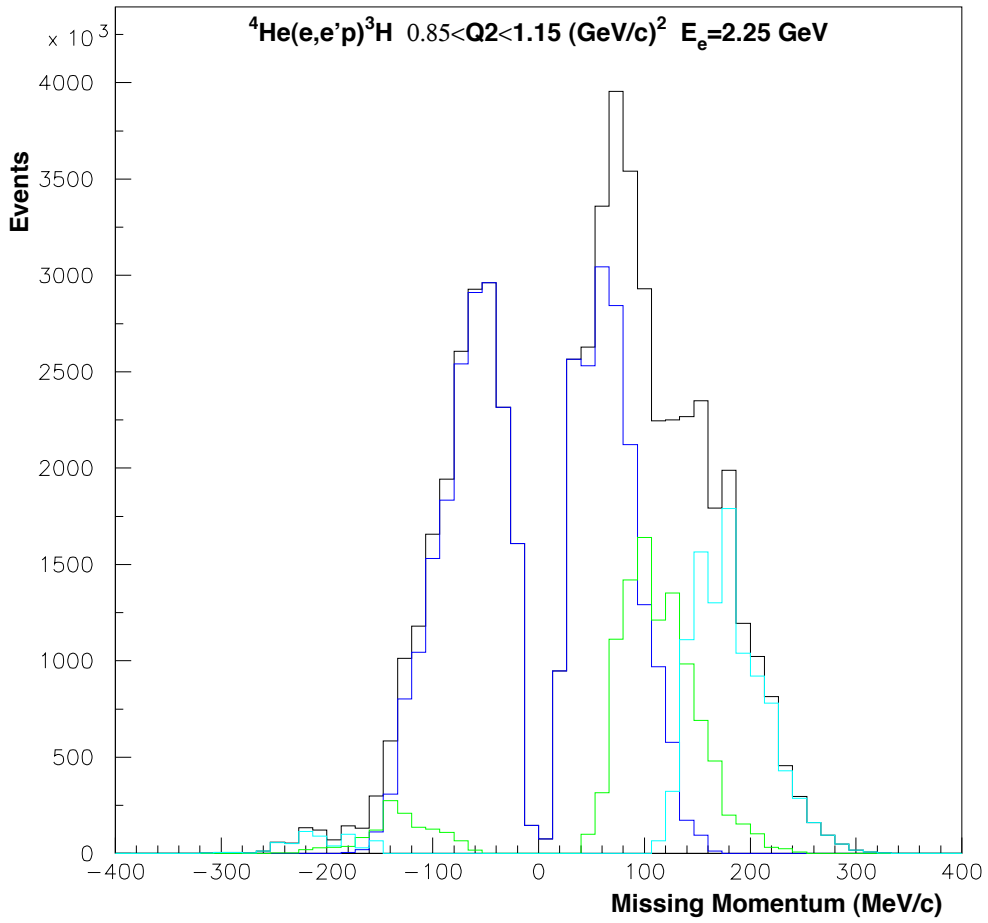

FIG. 11. Simulated $^4\mathrm{He}(e,e'p)^3\mathrm{H}$ coverage in missing momentum for the $Q^2 = 1.0$ $(\mathrm{GeV}/c)^2$ settings listed in Table I. The kinematic coverage of the respective HMS settings are indicated by color: Blue: $p_m = 0$, Green: $p_m = +0.140$ MeV/c, Cyan: $p_m = +0.220$ MeV/c, Black: sum of all 3 settings. All acceptance cuts listed in the text, as well as a missing mass cut to select the $t + p$ final state, and a cut on Q^2, are applied.

$^1H(e,e'p)$ *Scans* We propose to acquire scans of hydrogen elastic scattering events at $Q^2 = 1.0$, and 1.8 $(\mathrm{GeV}/c)^2$. As shown in Fig. 12, seven settings of HMS momentum, from $\delta_{\mathrm{HMS}} = -11.1\%$ to $+12.5\%$ will provide good coverage across the HMS focal plane. This will allow the instrumental asymmetries of the FPP to be studied, as well as to provide a reference for the polarization-transfer-ratio measurements.

C. Instrumentation

Spectrometers This experiment requires a maximum HMS momentum of 2.0 GeV/c, which is well within the region of well known HMS matrix elements. No HMS optics checks

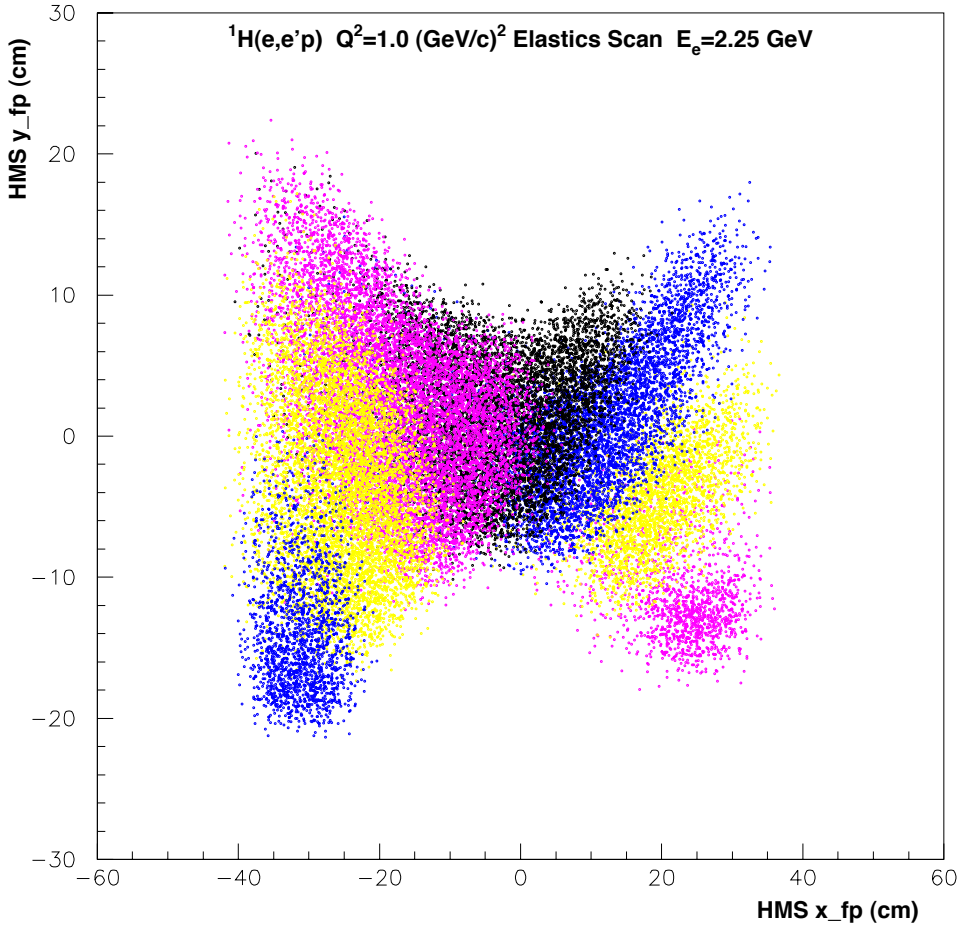

FIG. 12. Simulated ^{1}H$(e, e'p)$ focal plane scan for the $Q^2 = 1.0$ (GeV/c)^2 settings listed in Table I. The data are color coded according to the HMS momentum setting. Seven settings, from $\delta_{\rm HMS} = -11.1\%$ to $+12.5\%$ will provide good coverage across the HMS focal plane.

are planned. The experiment also requires the use of the SHMS up to a central momentum setting of 3.4 GeV/c, at relatively large angles $19.8^\circ < \theta_{SHMS} < 29.8^\circ$. In comparison to the planned SHMS characteristics, these are relatively modest demands, which should be suited for relatively early running – possibly as one of the SHMS commissioning experiments. We expect the initial SHMS commissioning procedure to meet the relatively modest demands of this experiment, and so we do not request beam time for additional SHMS optics checks.

Target The use of hydrogen, deuterium and ^{4}He cryogenic targets are proposed for this experiment. Since only two cryo-targets are typically mounted on the ladder at a time, the necessity to switch from ^{1}H to ^{2}H at each beam energy will cause some downtime estimated at 12 hours per change. This downtime has been included as one of the configuration changes in the beam request in Table V. Since the scattered electron angle is no larger than 30°, our rate estimates assume the use of an 8 cm cryotarget. Several approved HMS+SHMS

experiments also assume the use of an 8 cm cryotarget, so we expect this to be one of the standard target cell geometries to be available after the upgrade. The target windows will be viewed by both spectrometers at most angle settings, so target empty measurements must also be made. We expect the resulting luminosity and rate to be well within the operational experience of previous Hall C standard equipment experiments.

Beam The standard Hall C beamline hardware will be used. In addition to the raster systems, super-harps permit accurate measurements of beam size and angle. The Hall C Moller Polarimeter measures the polarization of the electron beam arriving in Hall C. As shown in the following section, knowledge of the absolute beam polarization is required for the extraction of the polarization-transfer observables. The Hall C Moller operates by observing the rate of production of Moller electrons at 90° in the center of mass when the beam strikes a thin iron target. The outer shell electrons in the iron are polarized parallel (or anti-parallel) to the beam direction by a 4 T magnetic field. The Moller electron production rate differs when the beam and target electron spins are aligned parallel or anti-parallel to one-another. Measurement of this rate difference provides a measure of the beam polarization. The Hall C Moller Polarimeter is able to provide an absolute polarization measurement with an accuracy better than 1.5%. Typically, a beam polarization measurement can be carried out in about one hour (plus approximately one hour of setup overhead), and since the electron spin precession from the source to Hall C varies with beam energy, we plan to measure the beam polarization at the beginning of each kinematic setting (typically eight hours of calendar time overhead).

FPP As noted above, the polarization of the recoil proton will be measured in the Focal Plane Polarimeter (FPP) which has been previously installed in the detector shield house of the HMS in Hall C for the GEp-III and GEp-2γ experiments. In its current configuration, the FPP consists of two (passive) CH_2 analyzer blocks in series, with each one followed by two drift multiwire chambers with a sensitive area of 2.06 m^2; it is shown installed in the HMS detector hut in Fig. 13.

At the proton momenta considered in this experiment, the double polarimeter configuration results in typical efficiencies (*i.e.* the number of incident protons that nuclear scatter in either CH_2 block at a significant polar angle and are detected in the corresponding wire chamber pair) for single track events of approximately 40-45%. In the GEp-III and GEp-2γ experiments, it was determined that clear identification of single track events led to the highest coefficient of merit for the polarimeter, as multi-track events are seen to have significantly reduced analyzing power. As it will provide a benefit to not only this experiment, but also for other experiments which plan to use the FPP in Hall C following the upgrade, the current plan is to enhance the tracking capability of the existing FPP chambers by adding extra tracking planes (through the efficient redistribution of planes from a spare chamber that has already been constructed). In addition to enhancing the overall tracking efficiency of the FPP, it is expected that this will also significantly reduce instrumental uncertainties in the device, which is of benefit in the extraction of the induced polarization, P_y.

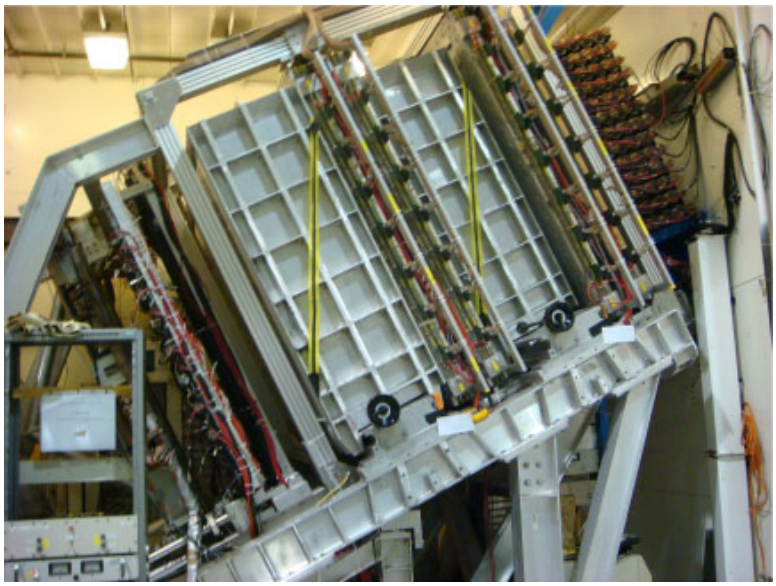

FIG. 13. The Focal Plane Polarimeter (FPP) installed in the Hall C HMS detector hut.

For this experiment, because of the relatively low proton momentum in the HMS, the thickness of CH_2 in each analyzer will need to be reduced at some kinematic settings. Moreover, installation of the FPP in the HMS detector hut requires the removal of the second layer of triggering scintillators (the so-called "S2" layer). To compensate for this, for the Gep-III/Gep-2γ experiments, a new scintillator detector (known as "S0") was constructed and installed in the space between the exit window of the HMS spectrometer and the HMS wire chambers. At the relatively high proton momenta of these experiments, the multiple scattering is small in S0, and thus HMS tracking is not significantly affected. However, for the current experiment, this will not be the case. In addition, the S0 detector was constructed to detect primarily elastic protons in scattering from hydrogen, which are confined to a narrow region of the focal plane in the HMS. Therefore, it is simply not large enough to cover the entire focal plane of the HMS, as is required in this proposal.

Thus, we are proposing to construct a new CH_2 analyzer system, which will allow for varying CH_2 thickness, as required for this experiment, and will also serve as an additional trigger layer. For this experiment, we require three thicknesses of analyzer – 5 cm, 20 cm, and 40 cm – to optimize the scattering efficiency in the FPP at the various momentum settings of the HMS. To allow for this optimization, each FPP analyzer will consist of a "passive" CH_2 part, and an "active" scintillator layer, which will provide an additional trigger layer for the experiment, and will also serve as analyzer material. The passive part of each analyzer will consist of "split" CH_2 blocks (to allow for straight-though track calibrations) which will be similar in design to the current system. Each analyzer in the FPP will have two sets of 20 cm-thick blocks. In addition, each analyzer will have an active scintillator layer (behind the passive CH_2 analyzer), consisting of ten (5 cm thick $\times$ 15 cm high) horizontal (*i.e.* x-direction) scintillators. Incidentally, we plan to use the

TABLE II. HMS focal plane polarimeter CH_2/scintillator layer configurations for the range of HMS proton momenta in the experiment. FPP1 and FPP2 refer to the first and second analyzers of the polarimeter, respectively.

Proton Momentum	FPP1		FPP2	
Range (GeV/c)	CH_2 (cm)	Scint. (cm)	CH_2 (cm)	Scint. (cm)
0.700 – 0.900	20.0	5.0	-	5.0
0.900 – 1.125	40.0	5.0	-	5.0
1.125 – 1.300	40.0	5.0	20.0	5.0
Above 1.300	40.0	5.0	40.0	5.0

existing HMS S2 scintillator readout electronics for the two new scintillator layers. The specific configuration of the analyzers for the range of HMS proton momenta required in this experiment is given in Table II.

The azimuthal distribution of the protons which undergo a second scattering in the analyzer depends upon the proton polarization due to the spin-orbit part of the strong nuclear force [64]. The degree of polarization is directly related to the asymmetry of this angular distribution by:

$$N_p(\theta,\phi) = N_p\Big[1 + (a_i + A_y(\theta)P_y^{fp})\sin\phi + (b_i - A_y(\theta)P_x^{fp})\cos\phi\Big], \tag{3}$$

where N_p is the number of protons incident on the polarimeter which scatter into a given angular range, and a_i and b_i parameterize instrumental asymmetries. Empirically, the analyzing power, A_y, is the amplitude, A, of the asymmetry resulting from the scattering of a particle with polarization, P_y, i.e. $A_y = \frac{A}{P_y}$. Based on previous experiments (at JLab and elsewhere), the maximum analyzing power has been found to be proportional to $1/p$, the inverse of the proton momentum, over a large range of proton momenta. It is also true that A_y^{max} occurs at a fixed value of the transverse momentum transfer, $p_T = p\sin(\vartheta_{fpp}) \simeq 0.3$ GeV/c. Finally, the shape of the analyzing power distribution as a function of ϑ is largely independent of momentum. These ideas together allow us to obtain reliable predictions for the analyzing power distributions for all of the proton momenta in the experiment.

In terms of determining the expected uncertainties in the measured polarization observables, the crucial feature of the polarimeter is its coefficient of merit (COM), defined as COM=$\int_{\vartheta_{min}}^{\vartheta_{max}} \epsilon(\vartheta)A_y^2(\vartheta)d\vartheta \sim \epsilon A_y^2$, where $\epsilon(\vartheta)$ is the differential fraction of events scattered in the analyzer at polar angle ϑ. The differential scattering fraction has been estimated from a full Geant3-based simulation of the polarimeter. Estimates obtained for the scattering fraction from this simulation are in good agreement with the results of previous experiments, including the recent Gep-III/Gep-2γ experiments in Hall C. Thus, we are confident in our estimates for this new experiment.

As the proton travels through the HMS, its spin precesses due to the interaction of the magnetic moment of the proton with the magnetic elements of the HMS, which consists of a series of quadrupole magnets as well as the principal vertical bend dipole magnet.

The proton polarization at the spectrometer focal plane is related to its polarization at the target by a spin matrix:

$$\begin{pmatrix} \mathbf{P_x^{fp}} \\ \mathbf{P_y^{fp}} \\ P_z^{fp} \end{pmatrix} = \begin{pmatrix} S_{xx} & \mathbf{S_{xy}} & \mathbf{S_{xz}} \\ S_{yx} & \mathbf{S_{yy}} & \mathbf{S_{yz}} \\ S_{zx} & S_{zy} & S_{zz} \end{pmatrix} \begin{pmatrix} P_x^{tar} \\ \mathbf{P_y^{tar}} \\ \mathbf{P_z^{tar}} \end{pmatrix} \tag{4}$$

The focal plane polarimeter measures only the transverse and normal, P_y^{fp} and P_x^{fp}, components of the proton polarization. The spin matrix is calculated using a model of the spectrometer with the differential-algebra-based transport code COSY. Details are given in Ref. [65] regarding the method for extracting the target polarizations from the knowledge of the spin matrix and measurement of the $N(\theta, \phi)$ distributions. For a standard QQQD magnet spectrometer, the spin matrix components, S_{xx}, S_{yx}, and S_{yz}, are almost zero when averaged over the phase space, and thus for the HMS spectrometer, the systematic uncertainties due to spin precession are expected to be relatively small. In addition, for the purposes of calculating projected uncertainties for this experiment, it is an excellent approximation to consider spin precession in the dipole magnet of the HMS only. In this case, the focal plane polarization components are written as:

$$P_x^{fp} = P_y^{tar} \cos\chi_{\rm HMS} \pm hP_z^{tar} \sin\chi_{\rm HMS} \tag{5}$$

$$P_y^{fp} = \pm hP_x^{tar} \tag{6}$$

where h is the electron beam polarization, and $\chi_{\rm HMS}$ is the spin precession angle in the dipole magnet of the HMS. The azimuthal angular distributions of the sum and difference of the two electron beam helicity states are then, respectively:

$$\frac{N_p^+(\theta,\phi) + N_p^-(\theta,\phi)}{2N_p} = 1 + a_i \sin\phi + \Big(b_i + A_y(\theta) P_y^{tar} \cos\chi_{\rm HMS}\Big) \cos\phi, \tag{7}$$

$$\frac{N_p^+(\theta,\phi) - N_p^-(\theta,\phi)}{2N_p} = hA_y(\theta) P_x^{tar} \sin\phi - hA_y(\theta) P_z^{tar} \sin\chi_{\rm HMS} \cos\phi. \tag{8}$$

The uncertainty in the Fourier components of these distributions is given by $\sqrt{\frac{2}{N_p}}$, where N_p is the number of protons which scatter in the analyzer in a given angular range. Thus, the uncertainties on the target polarizations are:

$$\sigma(P_x^{tar}) = \sqrt{\frac{2}{N_p h^2 A_y^2}}, \tag{9}$$

$$\sigma(P_y^{tar}) = \sqrt{\frac{2}{N_p A_y^2 \cos^2\chi_{\rm HMS}}}, \tag{10}$$

$$\sigma(P_z^{tar}) = \sqrt{\frac{2}{N_p h^2 A_y^2 \sin^2\chi_{\rm HMS}}}. \tag{11}$$

D. Rates

Our real-rate estimates are based on SIMC [66] Monte Carlo simulations of the Hall C spectrometers, incorporating the actual spectrometer acceptances and radiative effects. We also assume:

- Cryotarget cell diameter of 8 cm.
- Maximum beam current of 75 μA, with a polarization of 85%.
- DAQ rate up to $\sim$2 kHz with acceptable dead time.
- An average FPP scattering efficiency of 42%, and effective overall analyzing power given as 70% of the maximum analyzing power $A_y^{max} = 0.029 + 0.34(1/p)$, where p is the proton momentum in GeV/c. Both of these are determined from our analysis of the recent Gep-2γ data, together with GEANT simulations of the FPP.

The ^{4}He$(e,e'p)$ real coincidence rate estimates are based on a spectral function model of the form

$$S(p_{recoil}, E_{sep}) = S(p_{recoil})S(E_{sep})$$

where $S(p_{recoil})$ is the Urbana momentum distribution employed by MCEEP [67] for the two-body breakup channel ^{4}He$(e,e'p)^3$H and $S(E_{sep})$ is the ^{4}He$(e,e'p)$ missing energy distribution measured by Richard Florizone, et al. The real coincidence rates listed in Table III include no missing mass cuts, while the uncertainties shown in Figs 7, 8, and Table IV include the effect of spectrometer acceptance and missing mass cuts. The ^{2}H and ^{1}H real coincidence rates are based on parameterizations of existing data, as implemented in SIMC.

Singles rates in the HMS and SHMS were examined for $p(e,e'\pi^+)$ data taking [68], and are listed in Table III. The total singles rates are well below the capability of the detector packages, which were constructed with multi-MHz singles rates in mind. For the purpose of calculating online random coincidence rates, the HMS trigger rate is taken as equal to the raw trigger rate (we do not distinguish pions and protons in the HMS online). The SHMS trigger rate is taken as due to electrons only, since our calculations project raw π^- rates under 100 Hz, which should be further reduced by an expected online π^- rejection rate of 25:1. The random coincidence rate is then given by (HMS trigger rate)(SHMS trigger rate)Δt, where the coincidence resolving time Δt = 40 nsec. In all cases the expected reals:randoms coincidence rate ratio is expected to be at least 9:1. The real coincidence rate is particularly large for two ^{1}H, ^{2}H settings at Q^2 = 1.0 (GeV/c)^2. In these cases, the beam current used in the rate estimate was adjusted downwards to keep the resulting online real + random rates below $\sim$ 2 kHz. Reliable cross sections have been measured with the Hall C standard equipment and deadtimes $>$ 50%, which corresponds to a significantly higher rate than the upper limit assumed here. Offline, the relevant resolving time is 2 nsec and the reals to randoms ratio will be at the few percent level in all cases after further particle and channel identification cuts.

TABLE III. Projected SHMS and HMS rates from a 8 cm cryogenic target. The HMS+SHMS random coincidence rates $(e^-) \cdot (\pi^+ + p)$ assume a resolving time of 40 ns and no particle ID or missing mass cuts, thus corresponding to the online rate only; offline cuts will reduce this number to a few percent of the reals. In the case of the hydrogen elastics settings, only the highest rates of that setting are shown.

Tgt	p_m	I	SHMS Singles Rates		HMS Singles Rates		Random coinc.	Real coinc.
	(MeV/c)	(μA)	(kHz)		(kHz)		(Hz)	(Hz)
			e^-	π^-	π^+	p		
Q^2=1.0 (GeV/c)^2, E_e=2.250 GeV								
^{4}He	+0.220	75	6.1	0.06	1.0	5.9	1.7	23.7
	+0.140	75	2.3	0.06	3.3	13	1.5	121
	0.0	75	3.1	0.06	6.6	22	3.6	364
^{2}H	+0.220	75	14	0.02	4.0	16	11.2	21.4
	+0.140	75	18	0.02	14	25	28.1	268
	0.0	50	13	0.02	19	28	24.0	1675
^{1}H	0.0	25	8	0	5.4	0.4	1.8	2105
Q^2=1.8 (GeV/c)^2, E_e=4.400 GeV								
^{4}He	0.0	75	10	0.1	1.3	1.1	1.0	161
^{1}H	0.0	75	11	0	0.7	0.5	0.6	1405

E. Background

Once a combination of online hardware and offline software has determined that there was a coincidence between an electron in the SHMS and proton in the HMS, there remain several backgrounds of the incoherent 'non-physics' variety: random coincidences and events from the target endcaps.

The electronic coincidence resolving window will be roughly 40 nsec. Offline our excellent coincidence time resolution enables us to reduce the relevant resolving time to 2 nsec with negligible inefficiency. This is the first level of suppression of random coincidences.

The missing (or undetected residual) mass is reconstructed from the final electron and detected hadron 4-momenta:

$$m_m^2 = P_m^2 = (P_e - P_{e'} + P_{tgt} - P_p)^2$$

A histogram indicating the anticipated missing mass resolution is shown in Fig. 14. These missing mass simulations incorporate the spectral function model discussed in Sec. II D and radiative effects. We expect a ± 5 MeV cut around the ^{3}H missing mass (for the ^{4}He$(e, e'p)$

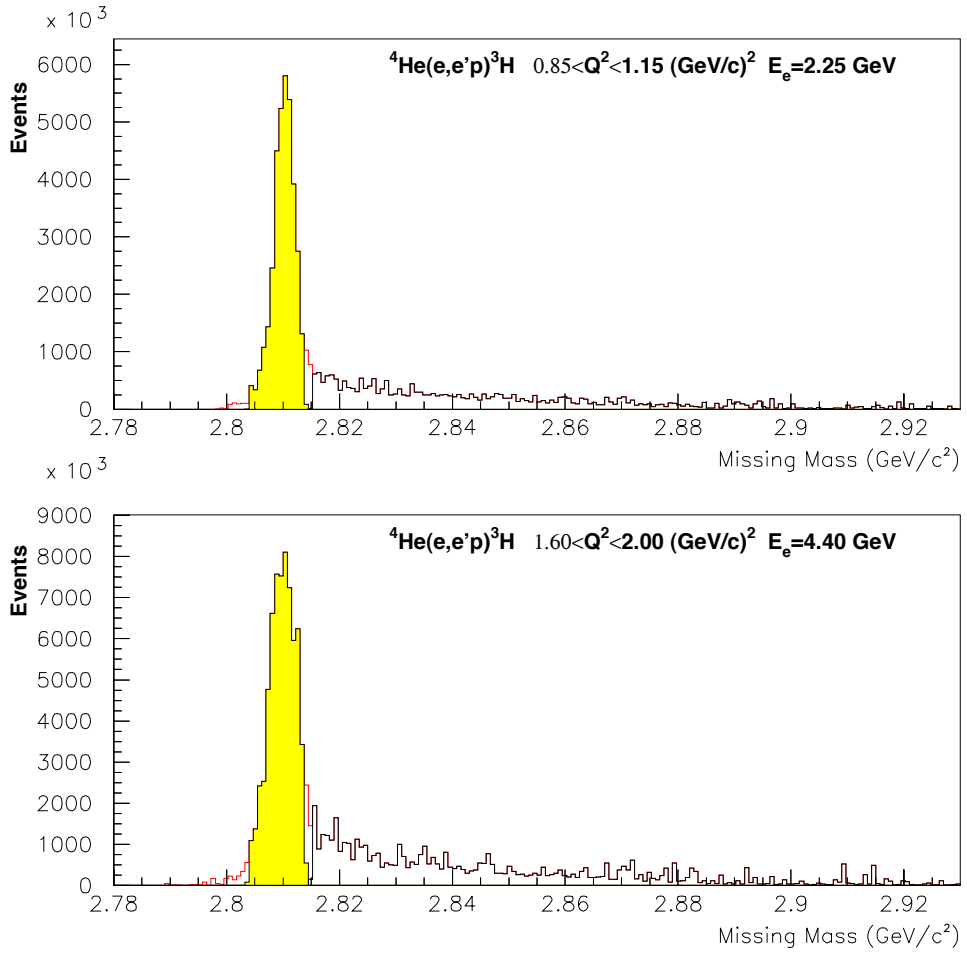

FIG. 14. Simulated reconstruction of the ^{3}H missing mass for the ^{4}He$(e, e'p)$ reaction. The yellow region indicates the applied missing mass cut used in the rate estimates of this proposal. All acceptance cuts listed in the text, and the indicated cuts on Q^2, are also applied.

data) to reduce the final random coincidence contamination to the few percent level.

Since SIMC sometimes underestimates the anticipated missing mass resolution, and the SHMS is only now being built, it is yet to be demonstrated that our measurement will achieve the missing mass resolution indicated in our simulations. However, even if the obtained missing mass resolution is $\sim 40\%$ than our simulations indicate, the experimental result should not be adversely affected. This is because previous ^{4}He$(\vec{e}, e'\vec{p})$ measurements indicate that the polarization transfer observables in the 'near breakup' region are the same (within uncertainties) as the ^{3}H peak. Therefore, we might even consider to broaden the missing mass cut to obtain extra statistics if the reals/accidentals ratio is favorable. HMS punch-through events also contribute to the missing mass tail, but typically 50-100 MeV higher than the exclusive peak. Since this far from any missing mass cut we would expect

to use, we have not included this effect in our rate simulations.

We also do not expect spin-dependent scattering in the target material to mimic any medium modification effects in ^{2}H and ^{4}He. Proton-nucleus scattering at small angles ($< 3^o$) is strongly dominated by Coulomb scattering, which is spin-independent, and protons with larger scattering angles will not meet the imposed kinematic constraints of quasi-elastic scattering with ^{3}H in the final state. In either case, spin-dependent scattering does not play a role in this experiment and has not been included in our simulations.

Finally, we have chosen the target length to be 8 cm. We expect that both spectrometers will view the end windows in all settings, making window background subtractions a necessity. Because the aluminum windows are each 4 mils thick, the ratio of protons in the windows to protons in the liquid hydrogen is about 10%. However, the surviving window background after cuts is typically found to be only 1%. The reduction from the naive 10% to the measured 1% is presumably due to a combination of final state interactions, SHMS y_{target} acceptance, and missing mass cuts. The Hall C "empty" target consists of two 40 mil thick aluminum windows separated by 8 cm, which can tolerate up to 30 μA. Thus, our "empty" data come in 4 times = (40 mil $\times$ 30 μA) /(4 mil $\times$ 75 μA) faster than window events on the real target. We have allocated an amount equal to 10% of the ^{4}He running time for these dummy target runs.

F. Uncertainties

A summary of the expected uncertainties for the low-missing-momentum portions of the proposed experiment at $Q^2 = 1.0$ and $Q^2 = 1.3$ (GeV/c)^2 is given in Table IV. For the expected uncertainties at larger values of proton virtuality see Fig. 8. The main quantity of interest in this experiment is the polarization double ratio, $(P'_x/P'_z)_{\rm A}/(P'_x/P'_z)_{\rm H}$. In forming this quantity, systematic errors largely cancel.

- The polarizations are ratio quantities reflecting a modulation of the ϕ-distribution relative to the flat, unpolarized baseline. Therefore, polarizations are relatively insensitive to luminosity, global detector efficiencies and spectrometer solid angles.

- The helicity-dependent polarizations are determined by taking differences of the ϕ-distributions for left and right beam helicities. This has the effect of canceling the instrumental asymmetries for the polarization transfer observables to first order.

- The ratio P'_x/P'_z is independent of the polarimeter analyzing power and the beam polarization.

- The only significant experimental systematic uncertainty in the determination of the polarization ratio is the determination of the spin precession in the spectrometer. We estimate these uncertainties for P'_x/P'_z to be of the order ± 0.01. By further taking the ratio to the free case, $(P'_x/P'_z)_{\rm A}\,/(P'_x/P'_z)_{\rm H}$, the spin-precession errors partly cancel.

The extraction of P_y will require a greater degree of understanding of the apparatus, especially with respect to instrumental uncertainties. Dedicated ^{1}H$(e,e'\vec{p})$ elastic data allowed us to significantly reduce the systematic uncertainties in P_y in E03-104 compared to our previous measurements [45]. We the help of the proposed ^{1}H$(\vec{e},e'\vec{p})$ data we hope to achieve the same for the proposed experiment and obtain systematic uncertainties in P_y in the order of ± 0.01.

TABLE IV. Projected uncertainties for the induced polarization and polarization-transfer ratio in the $(\vec{e},e'\vec{p})$ reaction for ^{1}H elastic data and data on ^{2}H and ^{4}He, integrated over a missing momentum range of Δp_m. The systematic uncertainties for P_y are about 0.01, the systematic uncertainties for the ratio P'_x/P'_z are about 0.01; $\chi_{\rm HMS}$ is the average spin-precession angle.

$Q^2_{nominal}$	E_{beam}	$\chi_{\rm HMS}$	Δp_m	^{1}H	^{2}H		^{4}He	
(GeV$^2/c^2$)	(GeV)	(deg)	(MeV/c)	$\sigma(P'_x/P'_z)$	$\sigma(P_y)$	$\sigma(P'_x/P'_z)$	$\sigma(P_y)$	$\sigma(P'_x/P'_z)$
1.0	2.25	70.1	$\pm$100	0.0031	0.0041	0.0047	0.0048	0.0052
1.8	4.40	91.4	$\pm$175	0.0052	–	–	0.0727	0.0062

III. BEAM REQUEST

The beam request allows sufficient events to be acquired to measure the ^{4}He$(\vec{e},e'\vec{p})^3$H polarization-transfer double-ratios at $Q^2 = 1.0$ and 1.8 (GeV/c)^2 to $dR/R \approx 1-2\%$, see Fig. 7. Projected data for the ^{4}He$(\vec{e},e'\vec{p})^3$H and ^{2}H$(\vec{e},e'\vec{p})n$ polarization-transfer double-ratios for various proton virtuality bins at $Q^2 = 1.0$ (GeV/c)^2 are shown in Figs. 8. Our overhead assumes 8 hours per beam energy change and an additional 12 hour overhead for a target configuration change at $Q^2 = 1.0$ (GeV/c)^2.

In addition, because the experiment requires only very modest SHMS capabilities, P_{SHMS} <3.5 GeV/c, and $19.8^\circ < \theta_{SHMS} < 29.8^\circ$, our measurement is a good candidate for relatively early running – possibly as one of the SHMS commissioning experiments.

A summary of the beam request is given in Table V.

[1] S. A. Moszkowski and B. L. Scott, Annals Phys. **11**, 65 (1960).

[2] R. D. Pisarski, Phys. Lett. **B110**, 155 (1982).

[3] A.W. Thomas, private communication (2003).

[4] Jefferson Lab Experiment E89-008, D. Day and B. Filippone, co-spokespersons.

[5] Jefferson Lab Experiment E02-019, A. Lung, J. Arrington, D. Day, and B. Filippone, co-spokespersons.

[6] Jefferson Lab Experiment E03-103, J. Arrington and D. Gaskell, co-spokespersons.

[7] J. Seely *et al.*, Phys. Rev. Lett. **103**, 202301 (2009), arXiv:0904.4448 [nucl-ex].

TABLE V. Beam request for deuterium and helium data taking, as well as hydrogen calibrations and dummy-target runs. We require high electron-beam polarization throughout. These numbers do not include the Hall plus equipment data-taking efficiency factor.

Target	E_e (GeV)	p_m (GeV/c)	Current (μA)	Real coinc. (Hz)	Time (hr)
$Q^2 = 1.0$ (GeV/c)^2 Settings					
^{4}He	2.250	+0.220	75	23.7	250
		+0.140	75	121	48
		0.0	75	364	48
^{2}H	2.250	+0.220	75	21.4	150
		+0.140	75	268	16
		0.0	50	1675	6
^{1}H	2.250	0.0	25	2105	7×3.0
Dummy	2.250	+0.220	30	9.5	25
		+0.140	30	49	5
		0.0	30	146	5
Overhead					20
Subtotal:					594 hr
$Q^2 = 1.8$ (GeV/c)^2 Settings					
^{4}He	4.400	0.0	75	161	225
^{1}H	4.400	0.0	75	1405	7×6.0
Dummy	4.400	0.0	30	65	23
Overhead					8
Subtotal:					298 hr
Grand Total:					892 hr (37 days)

[8] M. M. Sargsian *et al.*, J. Phys. **G29**, R1 (2003), arXiv:nucl-th/0210025.

[9] G. A. Miller and J. R. Smith, Phys. Rev. **C65**, 015211 (2002), arXiv:nucl-th/0107026.

[10] D.-H. Lu, A. W. Thomas, K. Tsushima, A. G. Williams, and K. Saito, Phys. Lett. **B417**, 217 (1998), arXiv:nucl-th/9706043.

[11] D.-H. Lu, K. Tsushima, A. W. Thomas, A. G. Williams, and K. Saito, Phys. Rev. **C60**, 068201 (1999), arXiv:nucl-th/9807074.

[12] M. R. Frank, B. K. Jennings, and G. A. Miller, Phys. Rev. **C54**, 920 (1996), arXiv:nucl-th/9509030.

[13] U. T. Yakhshiev, U.-G. Meissner, and A. Wirzba, Eur. Phys. J. **A16**, 569 (2003), arXiv:nucl-th/0211055.

[14] J. R. Smith and G. A. Miller, Phys. Rev. **C70**, 065205 (2004), arXiv:nucl-th/0407093.

[15] T. Horikawa and W. Bentz, Nucl. Phys. **A762**, 102 (2005), arXiv:nucl-th/0506021.

[16] I. C. Cloet, G. A. Miller, E. Piasetzky, and G. Ron, Phys. Rev. Lett. **103**, 082301 (2009), arXiv:0903.1312 [nucl-th].

[17] W. Wen and H. Shen, Phys. Rev. **C77**, 065204 (2008), arXiv:0806.0504 [nucl-th].

[18] D.-H. Lu, A. W. Thomas, and K. Tsushima, (2001), arXiv:nucl-th/0112001.

[19] K. Tsushima, H.-c. Kim, and K. Saito, Phys. Rev. **C70**, 038501 (2004), arXiv:nucl-th/0307013.

[20] S. Liuti, (2006), arXiv:hep-ph/0601125.

[21] V. Guzey, A. W. Thomas, and K. Tsushima, Phys. Lett. **B673**, 9 (2009), arXiv:0806.3288 [hep-ph].

[22] V. Guzey, A. W. Thomas, and K. Tsushima, Phys. Rev. **C79**, 055205 (2009), arXiv:0902.0780 [hep-ph].

[23] J. Jourdan, Phys. Lett. **B353**, 189 (1995).

[24] J. Morgenstern and Z. E. Meziani, Phys. Lett. **B515**, 269 (2001), arXiv:nucl-ex/0105016.

[25] J. Carlson, J. Jourdan, R. Schiavilla, and I. Sick, Phys. Lett. **B553**, 191 (2003).

[26] I. Sick, Comments Nucl. Part. Phys. **A18**, 109 (1988).

[27] T. E. O. Ericson and A. Richter, Phys. Lett. **B183**, 249 (1987).

[28] J. W. Van Orden, Phys. Rev. **C74**, 034607 (2006), arXiv:nucl-th/0605031.

[29] A. I. Akhiezer and M. P. Rekalo, Sov. J. Part. Nucl. **4**, 277 (1974).

[30] R. G. Arnold, C. E. Carlson, and F. Gross, Phys. Rev. **C23**, 363 (1981).

[31] M. K. Jones *et al.* (Jefferson Lab Hall A), Phys. Rev. Lett. **84**, 1398 (2000), arXiv:nucl-ex/9910005.

[32] O. Gayou *et al.*, Phys. Rev. **C64**, 038202 (2001).

[33] O. Gayou *et al.* (Jefferson Lab Hall A), Phys. Rev. Lett. **88**, 092301 (2002), arXiv:nucl-ex/0111010.

[34] G. Ron *et al.*, Phys. Rev. Lett. **99**, 202002 (2007), arXiv:0706.0128 [nucl-ex].

[35] A. J. R. Puckett *et al.* (Gep-III Collaboration), Phys. Rev. Lett. **104**, 242301 (2010), arXiv:1005.3419 [nucl-ex].

[36] J.-M. Laget, Nucl. Phys. **A579**, 333 (1994).

[37] S. Malov *et al.*, Phys. Rev. **C62**, 057302 (2000).

[38] D. Eyl *et al.*, Z. Phys. **A352**, 211 (1995).

[39] B. D. Milbrath *et al.* (Bates FPP), Phys. Rev. Lett. **80**, 452 (1998), arXiv:nucl-ex/9712006.

[40] D. H. Barkhuff *et al.*, Phys. Lett. **B470**, 39 (1999).

[41] B. Hu *et al.*, Phys. Rev. **C73**, 064004 (2006), arXiv:nucl-ex/0601025.

[42] S. Dieterich *et al.*, Phys. Lett. **B500**, 47 (2001), arXiv:nucl-ex/0011008.

[43] S. Strauch *et al.* (Jefferson Lab E93-049), Phys. Rev. Lett. **91**, 052301 (2003), arXiv:nucl-ex/0211022.

[44] M. Paolone *et al.*, Phys. Rev. Lett. **105**, 072001 (2010), arXiv:1002.2188 [nucl-ex].

[45] S. P. Malace, M. Paolone, S. Strauch, *et al.* (The Jefferson Lab E03-104 Collaboration), Submitted to Phys. Rev. Lett. (2010), arXiv:1011.4483 [nucl-exp].

[46] R. Schiavilla, O. Benhar, A. Kievsky, L. E. Marcucci, and M. Viviani, Phys. Rev. Lett. **94**, 072303 (2005), arXiv:nucl-th/0412020.

[47] J. M. Udias, J. A. Caballero, E. Moya de Guerra, J. E. Amaro, and T. W. Donnelly, Phys. Rev. Lett. **83**, 5451 (1999), arXiv:nucl-th/9905030.

[48] J. A. Caballero, T. W. Donnelly, E. Moya de Guerra, and J. M. Udias, Nucl. Phys. **A632**, 323 (1998), arXiv:nucl-th/9710038.
[49] J. M. Udias and J. R. Vignote, Phys. Rev. **C62**, 034302 (2000), arXiv:nucl-th/0007047.
[50] P. Lava, J. Ryckebusch, B. Van Overmeire, and S. Strauch, Phys. Rev. **C71**, 014605 (2005), arXiv:nucl-th/0407105.
[51] C. J. Horowitz, Phys. Rev. **C31**, 1340 (1985).
[52] D. P. Murdock and C. J. Horowitz, Phys. Rev. **C35**, 1442 (1987).
[53] J. A. McNeil, L. Ray, and S. J. Wallace, Phys. Rev. **C27**, 2123 (1983).
[54] J.M. Udias, private communication (2010).
[55] T. De Forest, Nucl. Phys. **A392**, 232 (1983).
[56] R. J. Woo *et al.*, Phys. Rev. Lett. **80**, 456 (1998).
[57] J. Gao *et al.* (Jefferson Lab Hall A), Phys. Rev. Lett. **84**, 3265 (2000).
[58] A. Meucci, C. Giusti, and F. D. Pacati, Phys. Rev. **C66**, 034610 (2002), arXiv:nucl-th/0205055.
[59] J. J. Kelly, Phys. Rev. **C60**, 044609 (1999), arXiv:nucl-th/9905024.
[60] M. M. Sargsian, Phys. Rev. **C82**, 014612 (2010), arXiv:0910.2016 [nucl-th]; M.M. Sargsian, private communication (2010).
[61] C. Ciofi degli Atti, L. L. Frankfurt, L. P. Kaptari, and M. I. Strikman, Phys. Rev. **C76**, 055206 (2007), arXiv:0706.2937 [nucl-th].
[62] S. Jeschonnek and J. W. Van Orden, Phys. Rev. **C81**, 014008 (2010), arXiv:0911.3629 [nucl-th]; Phys. Rev. **C78**, 014007 (2008), arXiv:0805.3115 [nucl-th].
[63] The SHMS angular range is restricted to $< 40^\circ$.
[64] E. Aprile-Giboni *et al.*, Nucl. Instrum. Meth. **215**, 147 (1983).
[65] V. Punjabi *et al.*, Phys. Rev. **C71**, 055202 (2005), arXiv:nucl-ex/0501018.
[66] N.C.R. Makins, T.G. O'Neill, and many others, SIMC, Hall C Simulation Package, September 2006 Program Version.
[67] P. Ulmer, MCEEP, Monte Carlo for Electro-Nuclear Coincidence Experiments, Program Version 3.4 (2000).
[68] J. O'Connell and J. Lightbody, Comp. in Phys. **57** (1988), Electron rates: Program QFS, Hadron rates: Program EPC.